Title
Detection of luminescent single ultrasmall silicon nanoparticles using fluctuation correlation spectroscopy

Journal
Applied Physics Letters, 76(14)

ISSN
0003-6951

Authors
Akcakir, O
Therrien, J
Belomoin, G
et al.

Publication Date
2000-04-03

DOI
10.1063/1.126191

Detection of luminescent single ultrasmall silicon nanoparticles using fluctuation correlation spectroscopy

O. Akcakir, J. Therrien, G. Belomoin, N. Barry, J. D. Muller, E. Gratton, and M. Nayfeh[a)]
Department of Physics, University of Illinois at Urbana-Champaign, Urbana, Illinois 61801

(Received 1 November 1999; accepted for publication 11 February 2000)

We dispersed electrochemical etched Si into a colloid of ultrasmall blue luminescent nanoparticles, observable with the naked eye, in room light. We use two-photon near-infrared femtosecond excitation at 780 nm to record the fluctuating time series of the luminescence, and determine the number density, brightness, and size of diffusing fluorescent particles. The luminescence efficiency of particles is high enough such that we are able to detect a single particle, in a focal volume, of 1 pcm^3. The measurements yield a particle size of 1 nm, consistent with direct imaging by transmission electron microscopy. They also yield an excitation efficiency under two-photon excitation two to threefold larger than that of fluorescein. Detection of single particles paves the way for their use as labels in biosensing applications. © *2000 American Institute of Physics.* [S0003-6951(00)04814-2]

Electrochemical processes have been used to produce silicon with novel luminescence. The material was first prepared in the 1950s by electrochemical etching in hydrofluoric (HF) acid and ultraviolet (UV) irradiation,[1] but its red luminescence was discovered only in 1990 by Canham.[2] Recently we demonstrated the presence of micron-size regions that are rich in ultrasmall structures, for which the intensity of the luminescence has a threshold, and highly nonlinear emission characteristics, rising by several orders of magnitude in a stimulated emission process.[3] We developed an etching procedure that enriches the smaller substructure[4] and allows subsequent conversion into dispersed nanoparticles. Under UV excitation, intense blue emission is generated from the Si particle colloid, observable by the naked eye, in room light. We used two-photon fluctuation correlation spectroscopy and photon counting histogram (PCH) to analyze the fluctuations of the emission.[5] We demonstrated the detection of single Si particles, crossing the interaction volume of 1 pcm^3. The measurements yield a particle size of ~1 nm, consistent with direct imaging by transmission electron microscopy (TEM). They also yield an excitation efficiency two to threefold larger than that of fluorescein. Detection of single ultrasmall nanoparticles paves the way for their use as labels in biosensing.

The silicon substrates were (100) oriented, 1–10 Ω cm resistivity, *p*-type boron doped Si, laterally anodized in H_2O_2 and HF acid.[6] The peroxide catalyzes etching and cleans the material, resulting in much reduced structures of high chemical and electronic quality. The interaction of HF with silicon is a self limiting process since the interaction passivates with hydrogen. In anodization, the interaction is catalyzed by the external current. Incorporation of H_2O_2 catalyzes the process further because H_2O_2 oxidizes silicon while HF dissolves the oxide vigorously. The combined effect of the two chemicals leaves no oxygen and results also in hydrogen passivation of the material. The hydrogen passivation in this case is more complete and of better quality, and is free of electronic defects. Moreover, H_2O_2 is known to be the most powerful and commonly used oxidant to remove nearly every kind of contamination (organic material, metals, alkalines, and metal hydroxides) from silicon surfaces by oxidative dissolution and complex formation. The smallest structure is found where the anodizing current concentrates, such as at the meniscus (air–liquid interface).[7,8,3] The ultrasmall particles are enriched by advancing the wafer, at a speed of ~1 mm/h, producing a large meniscus-like area. An ultrasound acetone bath crumbles the top film into a colloid of ultrasmall particles, leaving a deep red luminescent bottom layer. Of the suspension, larger yellowish luminescent particles precipitate, leaving a stable luminescent bluish colloid. A thin graphite grid was coated with the particles. Direct imaging using high resolution TEM shows that the particles are 1 nm in diameter. Electron photospectroscopy showed that the particles are composed of Si with no oxygen present.[4]

We used mode locked femtosecond Ti–sapphire near infrared laser, generating pulses of 150 fs duration at a repetition rate of 80 MHz. At the target, the average power, 20 mW, is focused to a spot of 0.7 μm diameter using a 1.3 NA lens, giving an average intensity of $\sim 5\times 10^6$ W/cm^2 (peak pulse intensity of $\sim 4\times 10^{11}$ W/cm^2). The beam–sample interaction is viewed via an optical microscope (×40). Emission is detected in photon counting mode by either a photomultiplier with a relative detection efficiency of 20% and 50%, or by an avalanche photodiode (APD) with relative detection efficiency of 5% and 40% at 390 and 430 nm, respectively. The APD has a lower quantum efficiency at the particle emission wavelength, however, it has a lower dark count than the photomultiplier. When the colloid is excited by the pulsed 780 nm in a two-photon process, deep blue emission is observed via an optical microscope, with the naked eye, in room light. Also, when a colloid in a 1 cm cuvette is excited by the third harmonic of a Nd-YAG laser at 355 nm, deep blue luminescence is observed with the naked eye, in room light. The use of near infrared radiation in a two-photon process, however, is less damaging to the

a)Author to whom correspondence should be addressed; electronic mail: m-nayfeh@uiuc.edu

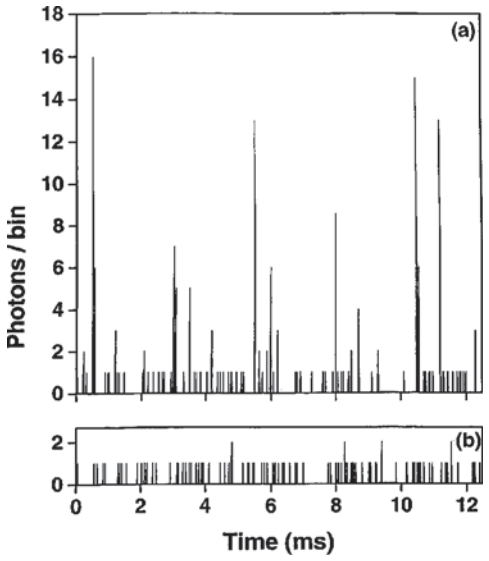

FIG. 1. Raw traces of (a) a Si particle sample and (b) a fluorescein standard, taken under the same intensity and beam focusing conditions.

sample, provides better discrimination against scattered incident radiation, as well as better definition of the probed volume. In multiphoton excitation processes, higher intensities are needed to induce excitation, thus the effective excitation volume is restricted to the central portion of the focal spot where the intensity is the highest, allowing fluctuating signals for nanomolar solutions of fluorophores to be detected.

Figures 1(a) and 1(b) gives sections of the photon counting time trace (binned in units of 12.5 ms) of emission of a Si colloid sample and a fluorescein standard, taken at an average intensity of 10^6 W/cm^2 at 780 nm, under the same beam focusing conditions. Fluorescein absorbs in a single photon process in the range 325–430 nm and emits in the range 450–600 nm. On the other hand, the particles absorb in the range 300–400 nm with a maximum absorption at 355 nm and emit in the range 390–460, with a maximum emission at 390 nm.[4] Unlike fluorescein, the nanocolloid traces show a number of events of significantly higher photon counting rate than the average rate.

We use a global procedure designed to analyze heterogeneous solutions of fluorophores, in which we concurrently analyze the amplitude of fluctuations as well as their persistence to yield the size, brightness, and number density. In the procedure, the analysis of amplitudes is achieved by the PCH method (frequency V s photon counts). The PCH measured within a suitable time window ($\sim$20 μs) for a nondiffusing single fluorophore yields a Poissonian distribution whose average yields a brightness parameter (incident intensity dependent). Diffusing fluorophores sample different regions of the excitation profile (e.g., three dimensional Gaussian). There will also be fluctuations in the number of particles detected. Averaging over the excitation profile and the number of fluorophores yields a super-Poissonian histogram. The deviation of the histogram from the ideal Poissonian contains information on the number density and effective brightness. Fitting routines allow these parameters to be extracted.[5] Analysis by the PCH method gives the histograms of the individual species comprising the sample as in Fig. 2 which shows that the majority events in the colloid average to a brightness ε_1 $\sim$0.1, with the number of particles in the focal volume N_1 is $\sim$30. But a small fraction $N_2/N_1 \sim 10^{-3}$ has an average brightness ε_2 as large as 50. The analysis gives one component for fluroescein as expected.

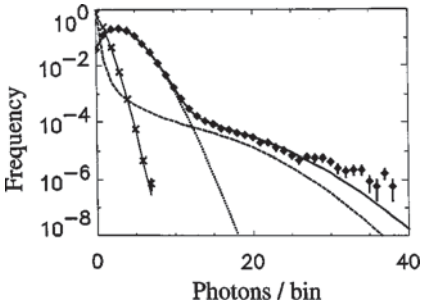

FIG. 2. Photon counting histogram (PCH) of the raw data of Fig. 1 showing the frequency of events versus photon per bin for (diamond) the particle sample and for (cross) fluorescein with (solid line) theoretical fits and the theoretical contribution (dot) of the majority particle species and (dash) of the minority particle species.

The diffusion coefficient (hence size) of the particles (as well as their number density) are determined, in the procedure, by calculating the autocorrelation function from the time series of photon counts. In the case of a single species, the autocorrelation function extrapolated to time zero gives the relative size of the fluctuation compared to the average signal. Dilute solutions yield higher relative fluctuations. The $t=0$ intercept is thus proportional to $1/N$ for a single species. Appropriate weighting must be used to evaluate the magnitude of relative fluctuations for multiple diffusing species. The diffusion coefficient of the particles on the other hand may be obtained by measuring the persistence of the fluctuation, which corresponds to the time a fluorophore requires to diffuse out of the focal volume, with smaller particles diffusing faster than larger ones. Figure 3 gives the autocorrelation function $\int I(t+\tau)I(t)^* dt$ for the particle sample of Fig. 1(a). We assume a Guassian beam profile and quadratic absorption dependence as measured. The correlation function is fitted to a two component Gaussian diffusion function: $G(t) = A_1[1/(1+8D_1t/w^2)] \times \mathrm{SQRT}[1/(1+8D_1t/z^2)] + A_2[1/(1+8D_2t/w^2)] \times \mathrm{SQRT}[1/(1+8D_2t/z^2)] + B$, where w is the

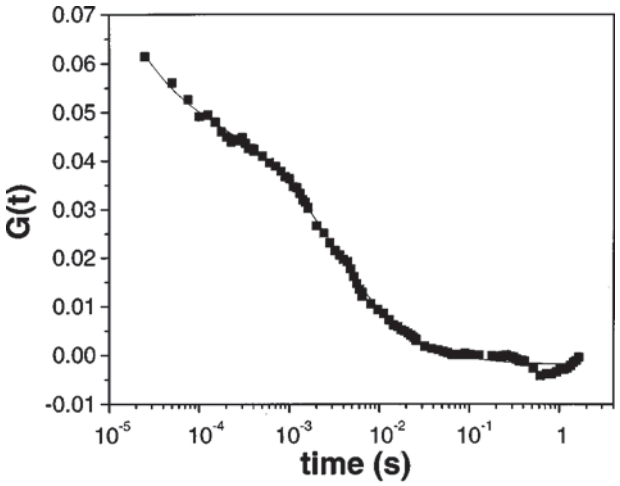

FIG. 3. Autocorrelation function $[G(t)]$ of the blue luminescence of the Si sample of Fig. 1a, along with a theoretical fit, yielding 29 particles in the focal volume.

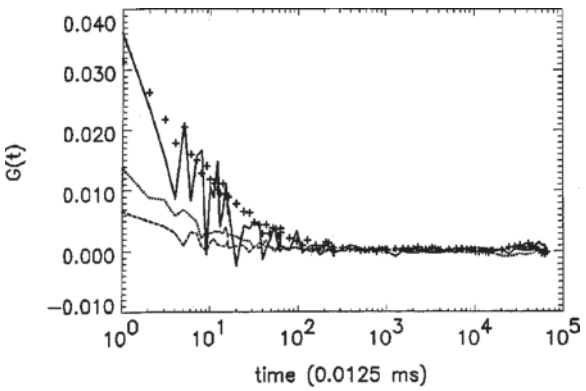

FIG. 4. Autocorrelation function $G(t)$ for (dash) a filtered Si particle sample with 5.4 particles in the focal volume (plus) the fluorescein standard with 1.5 molecule, (dot) a filtered Si samples with 2.8 particles and (solid) a filtered sample with less than a single particle (0.8) in the focal volume.

waist of the beam, z is the depth of the focal volume, t is time, I is the total average brightness, B is an offset, $A_i = 0.076 N_i (\varepsilon_1 / I)^2$, and N_i, ε_i, and D_i are the number of particles in the focal volume, brightness, and diffusion coefficient of the ith particle, $i = 1$ or 2, and 0.076 is a numerical calibration factor. From the response of fluorescein ($3 \times 10^{-6}\,\mathrm{cm}^2/\mathrm{s}$ diffusion coefficient), taken under the same beam focusing conditions, we get $w = 300\,\mathrm{nm}$ and $z = 2.5\,\mu\mathrm{m}$, or a volume of $0.68\ \mathrm{pcm}^3$. A self consistent analysis of the histogram and the autocorrelation spectra gives $N_1 = 29$, $\varepsilon_1 = 0.12$, $D_1 = 9.5 \times 10^{-6}\,\mathrm{cm}^2/\mathrm{s}$ for the majority component, and $N_2/N_1 = 8.6 \times 10^{-4}$, $\varepsilon_1 = 51$, and $D_2 = 11.4 \times 10^{-8}\,\mathrm{cm}^2/\mathrm{s}$ for the minority component.

Using the Stokes–Einstein relation, $d = kT/3\pi\eta D$, allows the size of the particles d to be estimated, where $T = 300\,\mathrm{K}$, the viscosity $\eta = 10^{-3}\,\mathrm{kg/m\,s}$, and k is the Boltzmann constant. This gives 0.9 and 80 nm for d, the particle diameter of the two components. The size of the majority species is consistent with direct high resolution TEM imaging.[4] Although the fitting procedure is reasonably accurate, we filtered the sample to remove the larger entities, hence simplify the analysis. The raw traces (not shown here) before and after filtering through a 200 nm filter show that the brightest events are dramatically reduced. Further filtering using a 10 nm filter demonstrated no detectable difference in the time traces. Since the luminosity of the larger entities is very high, we believe that they were actually clusters comprised of smaller luminescent particles.

We next recorded the time traces and the photon count histogram, and calculated the autocorrelation functions $G(t)$ for a filtered sample and a 10 nM fluorescein standard (Fig. 4, dash and cross, respectively) under the same beam conditions. A self consistent analysis, with the response being fitted to a single species, i.e., taking $A_2 = 0$ gives 5.4 particles and 1.4 fluorescein molecules in the focal volume, and a corresponding luminosity of 0.07 and 0.15. The count rate of a blank solvent is 200 counts/s, while 6500 counts/s is the count rate per silicon nanoparticle. With this signal to noise ratio, one can signal dilute samples such that one nanoparticle is found in the focal volume. To attain the single particle level, we diluted by factors of ~2 and ~5. We recorded the raw emission traces and the photon count histogram, and calculated the autocorrelation functions (see Fig. 4, dot and solid, respectively). A self consistent analysis gives 2.8 and less than one (0.8) particles for the dilution by factors of 2 and 5. The analysis gives luminosity of 0.083 and 0.081, respectively. When normalized, the autocorrelation functions of fluorescein and the particles are comparable, hence they have similar diffusion coefficient and size. Fluorescein molecules have a planar molecular structure of 8×8 atomic bonds (less than 1 nm across).

The excitation efficiency of the Si particles is now defined in terms of that of fluorescein. The quantum efficiency of fluorescein (emission efficiency per photon absorbed) is established at $90\% \pm 5\%$. The excitation efficiency presented here, however, is not the quantum efficiency; rather it is the product of absorption and quantum efficiencies. Using 0.078, the average luminosity of the measurements of the filtered sample and its dilution, gives an excitation efficiency 52% of the fluorescein standard (0.15). It should also be noted that the excitation and detection in these measurements are not optimized for the Si particles, rather they are skewed in favor of fluorescein. A rough estimate of the correction for the detector efficiency increases the excitation efficiency to a level two- to threefold larger then that of fluorescein. Moreover, the particle excitation efficiency is expected to increase for excitation at shorter wavelengths near its maximum response at 710 nm (by a factor of 4).

In conclusion, we demonstrated detection of a few ultrasmall (1 nm) silicon nanoparticles including single ones in a volume of 1 pcm^3. The particles were derived and dispersed in a colloid from porous silicon. Fluctuation correlation spectroscopy and photon counting histogram yield a diffusion coefficient, and a particle diameter comparable to those of the fluorescein molecule. The excitation efficiency (absorption times quantum efficiencies) was found to be two- to threefold larger than that of fluorescein. Using an infrared two photon process minimizes beam induced damage to biological systems, hence they have a great potential as fluorescent labels in biosensing.

The authors gratefully acknowledge the Center for Microanalysis of Materials, University of Illinois, which is supported by the US Department of Energy under Grant No. DEFG02-91-ER45439. They also thank the Laboratory of Fluorescence Dynamics (LFD) which is supported jointly by the National Institute of Health (Grant No. RR03155) and the University of Illinois at Urbana-Champaign.

[1] A. Uhlir, Bell Syst. Tech. J. **35**, 333 (1956).
[2] L. T. Canham, Appl. Phys. Lett. **57**, 1046 (1990); A. G. Cullis, L. T. Canham, and P. Calcott, J. Appl. Phys. **82**, 909 (1997).
[3] M. Nayfeh, O. Akcakir, J. Therrien, Z. Yamani, N. Barry, W. Yu, and E. Gratton, Appl. Phys. Lett. **75**, 4112 (1999).
[4] Z. Yamani, H. Thompson, L. AbuHassan, and M. H. Nayfeh, Appl. Phys. Lett. **70**, 3404 (1997); J. Therrien, G. Belomoin, and M. Nayfeh (unpublished).
[5] K. Berland, P. So, and E. Gratton, Biophys. J. **68**, 694 (1995); E. L. Elson and D. Magde, Biopolymers **13**, 1 (1974); J. D. Muller, Y. Chen, and E. Gratton, J. Biol. Phys. **78**, 474 (2000).
[6] D. Andsager, J. Hilliard, J. M. Hetrick, L. H. AbuHassan, M. Plisch, and M. H. Nayfeh, J. Appl. Phys. **74**, 4783 (1993); Z. Yamani, S. Ashhab, A. Nayfeh, and M. H. Nayfeh, *ibid.* **83**, 3929 (1998).
[7] Z. Yamani, N. Rigakis, and M. H. Nayfeh, Appl. Phys. Lett. **72**, 2556 (1998).
[8] Z. Yamani, O. Gurdal, A. Alaql, and M. Nayfeh, J. Appl. Phys. **85**, 8050 (1999).